Journal of Coordination Chemistry

ISSN: 0095-8972 (Print) 1029-0389 (Online) Journal homepage: http://www.tandfonline.com/loi/gcoo20

Benzoate-functionalized diiron propanedithiolate complexes with mono- and di-phosphine ligands as catalysts for reduction of protons

Chang-Gong Li, Feng Xue, Mao-Jin Cui & Jing-Yan Shang

To cite this article: Chang-Gong Li, Feng Xue, Mao-Jin Cui & Jing-Yan Shang (2015) Benzoate-functionalized diiron propanedithiolate complexes with mono- and di-phosphine ligands as catalysts for reduction of protons, Journal of Coordination Chemistry, 68:9, 1559-1570, DOI: 10.1080/00958972.2015.1026812

To link to this article: http://dx.doi.org/10.1080/00958972.2015.1026812

Accepted author version posted online: 09 Mar 2015.
Published online: 07 Apr 2015.

Journal of Coordination Chemistry, 2015
Vol. 68, No. 9, 1559–1570, http://dx.doi.org/10.1080/00958972.2015.1026812

Benzoate-functionalized diiron propanedithiolate complexes with mono- and di-phosphine ligands as catalysts for reduction of protons

CHANG-GONG LI*, FENG XUE, MAO-JIN CUI and JING-YAN SHANG

College of Chemistry & Chemical Engineering, Henan Institute of Science and Technology, Xinxiang, PR China

(*Received 30 August 2014; accepted 8 January 2015*)

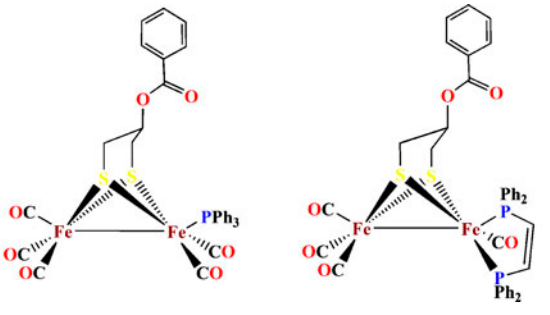

Reaction of the diiron propanedithiolate complex [μ-$(SCH_2)_2CHO_2CC_6H_5$]$Fe_2(CO)_6$ (**A**) with triphenylphosphine (PPh_3) or *cis*-1,2-bis(diphenylphosphine)ethylene (*cis*-dppv) in the presence of one equivalent of $Me_3NO{\cdot}2H_2O$ yielded a mono-substituted complex [μ-$(SCH_2)_2CHO_2CC_6H_5$]$Fe_2(CO)_5(PPh_3)$ (**1**) or an asymmetrically substituted complex [(μ-$SCH_2)_2CHO_2CC_6H_5$]$Fe_2(CO)_4(\kappa^2$-dppv) (**2**), respectively. The structures of both complexes were characterized by spectroscopic methods and X-ray crystallography. In the solid state, the PPh_3 ligand in **1** occupies an apical position of the square pyramidal geometries of the Fe2, while the *cis*-dppv in **2** coordinates Fe2 in an apical-basal manner. The electrochemistry of both complexes was investigated. The electron-withdrawing benzoate functionality on the bridgehead carbon of the propanedithiolate bridge shifts the oxidation and reduction potentials of **1** or **2** slightly. Both complexes can catalyze the reduction of protons from CF_3COOH but with a higher efficiency for **2**.

Keywords: [FeFe]-hydrogenase; Diiron dithiolate complex; Phosphine ligand; Crystal structure; Electrochemistry; Catalysis of reduction of protons

1. Introduction

Hydrogen is considered as a clean fuel which is efficient, renewable, and environmentally benign [1]. As a perfect energy, it can act as a candidate for dealing with urgent societal

*Corresponding author. Email: lichanggong@sohu.com

problems, such as diminishing fossil resources and deteriorating environment [2]. Fortunately, hydrogen can be produced by microbial hydrogenases with extremely high efficiency [3] and the structures and catalytic mechanism of [FeFe]-hydrogenases have been investigated by X-ray crystallography, FTIR and EPR spectroscopy [4–9]. The active sites of [FeFe]-hydrogenases consist of a $[Fe_2S_2]$ cluster joined with another $[Fe_4S_4]$ cluster by sulfur of a cysteinyl residue. The two irons of the $[Fe_2S_2]$ cluster are coordinated by CO and CN^- and are connected by a dithiolate SCH_2XCH_2S bridge (chart 1). A variety of models of the active sites of [FeFe]-hydrogenases have been synthesized in order to mimic the function and have insight into the biological system [10–14]. Among these models, propanedithiolate (pdt) complexes were widely studied due to the feasible modification at pdt bridge or ligand to other structural analogs for improvement of catalytic efficiency [15–17]. As a result, a series of hydroxyl [18–22], carboxyl [23–25], alkyl [26], phenyl [27], and ligand [28] functionalized diiron propanedithiolate complexes have been prepared. In addition, a theoretical investigation implemented by Tye, Darensbourg and Hall concluded that "asymmetric substitution of strong donor ligands is the most viable method of making synthetic diiron complexes that will serve as both structural and functional models"

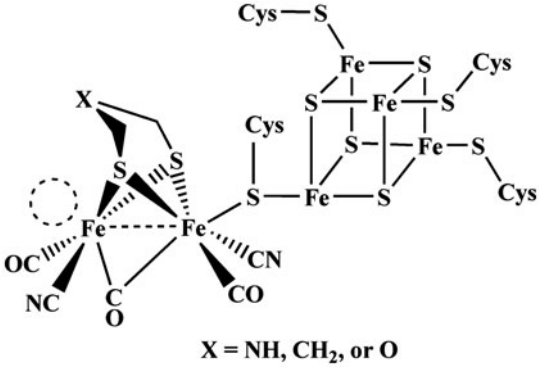

Chart 1. Basic structure of the active site obtained from protein crystallography.

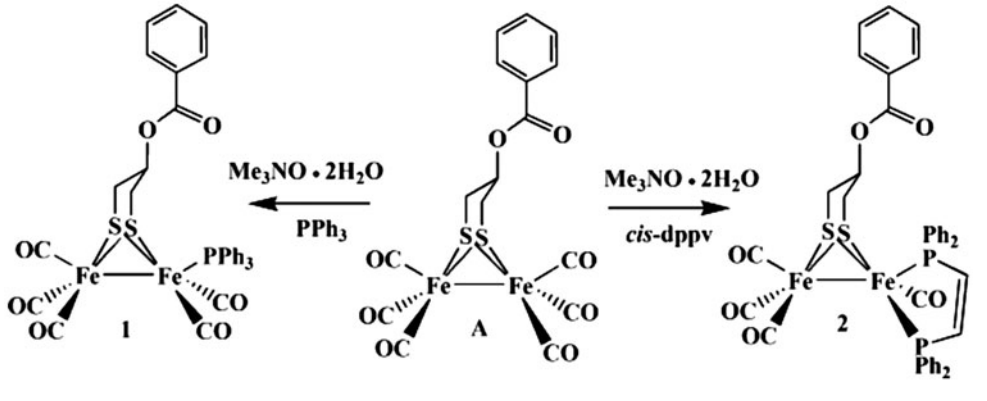

Scheme 1. Preparation of **1** and **2**.

of the active site of iron-only hydrogenase [29]. In this article, we report the synthesis, structural characterization, and electrocatalytic performance of the benzoate-functionalized diiron propanedithiolate complexes with mono- and di-phosphine ligands, investigating the influence of the benzoate function and the difference in asymmetry on the oxidation and reduction properties as well as the catalytic performance for the reduction of protons.

2. Experimental

2.1. *Materials and methods*

All reactions and operations were carried out under dry, oxygen-free argon using standard Schlenk, and vacuum line techniques. CH_2Cl_2 and MeCN were distilled over CaH_2, while *n*-hexane and toluene were distilled over sodium under argon. $Me_3NO{\cdot}2H_2O$, PPh_3, *cis*-dppv, and CF_3COOH were commercially available and used as received. Complex **A** was prepared according to literature method [19]. Preparative TLC was carried out on glass plates (25 cm × 20 cm × 0.25 cm) coated with silica gel G (10–40 μm). IR spectra were recorded on a Bruker TENSOR 27 FTIR spectrometer. ^1H, ^{13}C, and ^{31}P NMR spectra were obtained on a Bruker Avance 400 MHz spectrometer. Elemental analyses were performed on an Elementar Vario EL III analyzer.

2.2. *Electrochemistry*

Electrochemical measurements were carried out in a 10 mL one-compartment glass cell using a CHI 620 Electrochemical Workstation (CH Instruments, Chenhua, Shanghai, China). The electrolyte solution was 0.1 M *n*-Bu_4NPF_6 in MeCN purged with dry nitrogen for 10 min before measurement. CV scans were obtained in a three-electrode cell with a glassy carbon electrode (3 mm diameter) as the working electrode, successively polished with 3 and 1 μm diamond pastes and sonicated in ion-free water for 1 min, a platinum wire as the counter electrode, and a nonaqueous Ag/Ag^+ electrode (1.0 mmol $AgNO_3$ and 0.1 M *n*-Bu_4NPF_6 in MeCN) as reference. The potential scale was calibrated against the Fc/Fc^+ couple and reported *versus* this reference system.

2.3. *X-ray structure determination*

Single crystals of both complexes suitable for X-ray diffraction analysis were obtained by mixing *n*-hexane with a dichloromethane solution of **1** or **2** at 4 °C. For each complex, a suitable crystal was mounted on an Xcalibur, Eos, Gemini diffractometer. Data were collected at 291.15 K. Using Olex2 [30], the structures were solved with the ShelXS structure solution program using direct methods and refined with the ShelXL refinement package using least squares minimization [31].

2.4. *Synthesis and characterization of 1*

Parent complex **A** (126 mg, 0.25 mmol) was dissolved in dry MeCN (30 mL) under argon and then $Me_3NO{\cdot}2H_2O$ (28 mg, 0.25 mmol) was added. After stirring at room

temperature for 0.5 h, the resulting brown solution was mixed with PPh_3 (66 mg, 0.25 mmol) and stirred for 2 h at room temperature. The solvent was removed on a rotary evaporator and the residue was subjected to preparative TLC separation using CH_2Cl_2/petroleum ether (v/v = 2 : 3) as the eluent. From the main red band, **1** was obtained as a red solid (116 mg, 63%). IR (KBr disk, cm^{-1}): $\nu_{C\equiv O}$ 2041 (vs), 1985 (vs), 1944 (s), 1713 (m). ^1H NMR (400 MHz, $CDCl_3$, ppm): 1.510 (t, 2Ha, $^2J_{HaHe} = {}^3J_{HaHa'}$ = 12 Hz, 2 SCHaHe), 2.371 (dd, 2He, J_{HeHa} = 12 Hz, $J_{HeHa'}$ = 3.6 Hz), 3.737 (m, $1H_{a'}$, OCH), 7.254–7.773 (m, 20H, PhH). ^{13}C NMR (400 MHz, $CDCl_3$, ppm): 27.2 (SCH_2), 74.9 (OCH), 128.3, 128.5, 129.5, 129.7, 130.4, 133.1, 133.5, 133.6, 135.1, 135.6, 164.1 (PhC), 209.2, 213.6 (FeCO). ^{31}P NMR (161.9 MHz, $CDCl_3$, 85% H_3PO_4, ppm): 64.5 (s). Anal. Calcd for $C_{33}H_{25}Fe_2O_7PS_2$ (%): C, 53.54; H, 3.40. Found: C, 53.33; H, 3.46.

2.5. *Synthesis and characterization of 2*

Parent complex **A** (96 mg, 0.19 mmol) was dissolved in toluene (20 mL) under argon and $Me_3NO{\bullet}2H_2O$ (21 mg, 0.19 mmol) in MeCN (10 mL) was added. The red solution became brown immediately, after stirring at room temperature for *ca*. 15 min. A solution of *cis*-dppv (75 mg, 0.19 mmol) in toluene (10 mL) was added and the mixture was stirred at room temperature for 3 h. The solvent was removed on a rotary evaporator and the residue was subjected to preparative TLC separation using CH_2Cl_2/petroleum ether (v/v = 1 : 1) as eluent. From the brown band, **2** was obtained as a brown–black solid (139 mg, 87%). IR (KBr disk, cm^{-1}): $\nu_{C\equiv O}$ 2023 (vs), 1955 (vs), 1939 (vs), 1912 (s), 1707 (m). ^1H NMR (400 MHz, $CDCl_3$, ppm): 1.563 (t, 2Ha, $^2J_{HaHe} = {}^3J_{HaHa'}$ = 12 Hz, 2 SCHaHe), 2.649 (dd, 2He, J_{HeHa} = 9.2 Hz, $J_{HeHa'}$ = 3.2 Hz), 3.873 (m, $1H_{a'}$, OCH), 7.315–7.908 (m, 25H, PhH). ^{13}C NMR (400 MHz, $CDCl_3$, ppm): 28.8 (SCH_2), 75.3 (OCH), 128.2, 128.4, 129.4, 130.0, 130.4, 131.6, 132.9, 133.1, 134.9, 150.7, 151.1, 164.1 (PhC), 211.6 (FeCO). ^{31}P NMR (161.9 MHz, $CDCl_3$, 85% H_3PO_4, ppm): 96.4 (s, 73%, basal-apical), 79.8 (s, 27%, basal-basal). Anal. Calcd for $C_{40}H_{32}Fe_2O_6P_2S_2$ (%): C, 56.76; H, 3.81. Found: C, 57.03; H, 3.66.

3. Results and discussion

3.1. *Synthesis and spectroscopic characterization*

As shown in scheme 1, reaction of precursor **A** with one equivalent of PPh_3 or *cis*-dppv in the presence of one equivalent of $Me_3NO{\bullet}2H_2O$ yielded **1** or **2** in a moderate or high yield. In iron-containing mixed-metal clusters (μ_3-S)$FeCo_2(CO)_9$, the carbonyls bonded to cobalt are more easily exchanged by phosphine ligands than the carbonyls bound to iron without the decarbonylating reagent $Me_3NO{\cdot}2H_2O$ [32, 33]. The coordination of two ligands to one or two Fe atoms was decided initially by IR [34]. The highest absorption band of the terminal carbonyls of **1** (2041 cm^{-1}) or **2** (2023 cm^{-1}) indicated displacement of one carbonyl of parent complex **A** by PPh_3 in **1** [35] or two carbonyls by *cis*-dppv in a chelating manner in **2** [36–38], respectively. Upon comparison of IR spectra of **1** with that of [(μ-$SCH_2)_2CH_2$] $Fe_2(CO)_5(PPh_3)$ (2044 cm^{-1}), benzoate group on propanedithiolate bridge has a little influence on the electron density of diiron center, as do groups such as *p*-MeO-, *p*-Me- and *p*-F- in phosphine ligands in complexes [(μ-$SCH_2)_2CH_2$]$Fe_2(CO)_5$[P(Ph-R-*p*)$_3$] (R = *p*-OMe, *p*-Me or *p*-F) when using the IR of [(μ-$SCH_2)_2CH_2$]$Fe_2(CO)_5(PPh_3)$ as reference [39]. ^1H

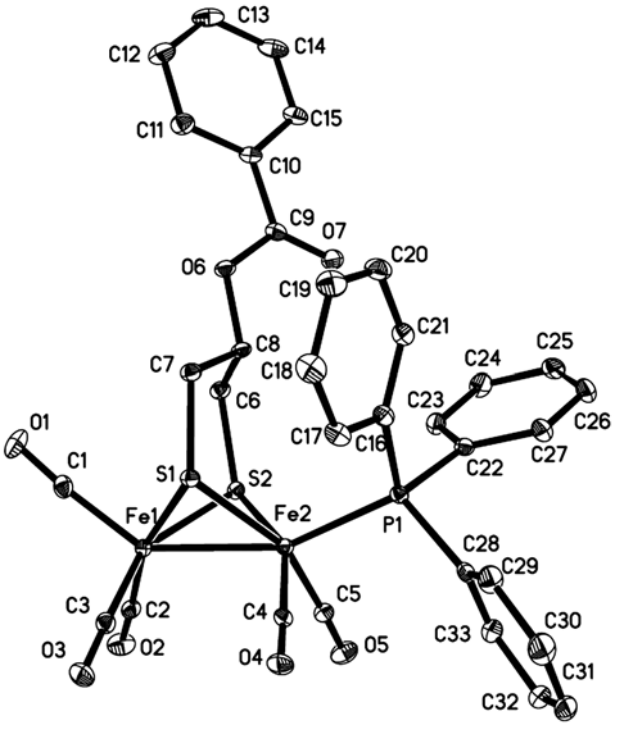

Figure 1. ORTEP view of **1** with 30% probability ellipsoids.

NMR spectra of **1** or **2** showed a multiplet at 3.737 or 3.873 ppm for the bridgehead C-attached axial hydrogen,[†] a doublet/doublet at 2.371 or 2.649 ppm for the equatorial hydrogens, and a triplet at 1.510 or 1.563 ppm for the axial hydrogens in two CH_2S groups [19]. Compared with those of parent complex **A**, the chemical shifts of protons on propanedithiolate bridges in **1** and **2** shifted up-field, consistent with the increment of electron density on their diiron centers caused by coordination of strong electron-donating ligands. The ^{31}P NMR spectra of **1** displayed one singlet at 64.5 ppm, whereas those of **2** showed two singlets at 96.4 and 79.8 ppm for the phosphorus atoms of *cis*-dppv ligand with a ratio of *ca.* 73 : 27 [36–38].

3.2. *X-ray crystal structures*

Crystals of **1** or **2** suitable for X-ray crystallography were grown upon slow mixing *n*-hexane with a saturated dichloromethane solution containing **1** or **2**. The ORTEP views of both complexes are displayed in figures 1 and 2 [40], while the crystal data and the selected metric data are given in tables 1 and 2, respectively. Each complex contains a Fe_2S_2 core with a benzoate functionality equatorially attached to the bridgehead carbon of the

[†]In a six-membered ring in chair conformation, axial hydrogen means that the C–H bond is perpendicular to the average plane of the six-membered ring, while equatorial hydrogen means that the C–H bond is approximately horizontal to the average plane of the six-membered ring.

propanedithiolate bridge [19]. The PPh_3 in **1** occupies an apical position of the square pyramid of Fe2, in accord with the analogous diiron propanedithiolate complexes with monophosphine ligand, such as $[(\mu\text{-}SCH_2)_2CH_2]Fe_2(CO)_5L$ (L = PPh_3, $P(OEt)_3$, $PhPMe_2$ [35], $Ph_2PNH(2\text{-}NH_2Ph)$, $Ph_2PNH(CH_2)_2NMe_2$, $Ph_2P(2\text{-}Me_2NCH_2Ph)$ [41], $Ph_2P(CH_2CO_2H)$ [42], and $Ph_2P(2\text{-}NHPy)$ [43]. The two phosphines of *cis*-dppv chelate one of the two irons with an apical-basal coordination geometry [36–38]. The bite angle P2–Fe2–P1 is 86.62(4)°, close to those of $[(\mu\text{-}SCH_2)_2]Fe_2(CO)_4(\kappa^2\text{-dppv})$ and $[(\mu\text{-}SCH_2)_2CHC_6H_5]Fe_2(CO)_4(\kappa^2\text{-dppv})$ [37, 38]. Two phosphorous atoms, two carbons of *cis*-dppv, and the Fe2 constitute a five-membered ring with dihedral angle of 19.5(1)° between the plane (P2, Fe2, P1) and the plane (P1, C17, C18). The four atoms, P1, C17, C18, and P2, are almost co-planar. The Fe–Fe bond lengths of **1** [2.5341(4) Å] and **2** [2.5472(7) Å] are longer than that in parent complex **A** [2.4973(8) Å].

3.3. *Electrochemistry*

The electrochemistry of **1** or **2** was studied in MeCN (figure 3). Complex **1** displayed an irreversible reduction at −1.721 V and an irreversible oxidation process at +0.395 V,

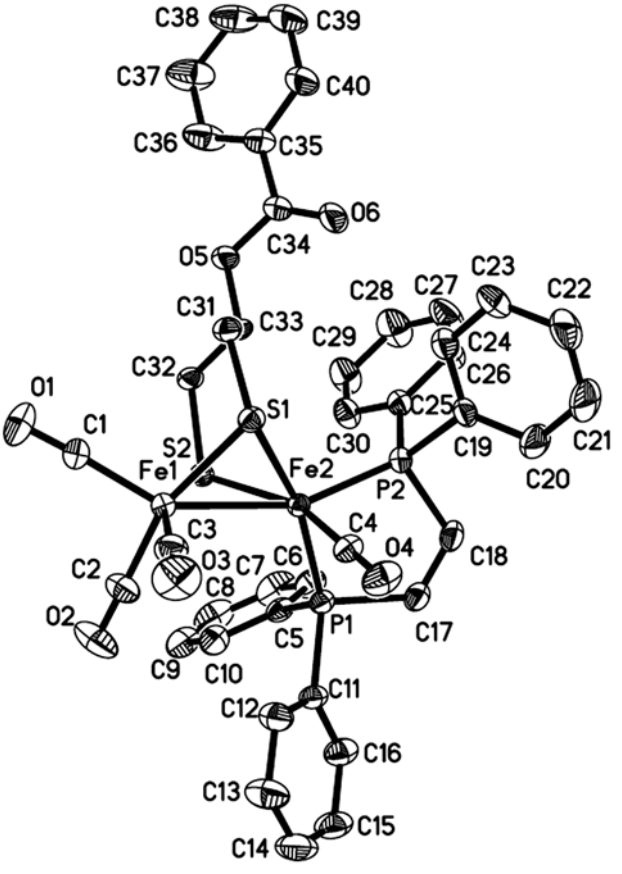

Figure 2. ORTEP view of **2** with 30% probability ellipsoids.

Table 1. Crystal data and structural refinements for **1** and **2**.

	1	**2**
Empirical formula	$C_{33}H_{25}Fe_2O_7PS_2$	$C_{40}H_{32}Fe_2O_6P_2S_2$
Formula weight	740.32	846.42
Crystal system	Orthorhombic	Triclinic
Space group	*Pbcn*	$P\bar{1}$
a (Å)	26.5845(7)	10.9485(6)
b (Å)	12.1795(3)	14.6354(8)
c (Å)	19.6959(5)	14.7545(8)
α (°)	90	118.370(5)
β (°)	90	105.858(5)
γ (°)	90	92.164(4)
V (Å^3)	6377.3(3)	1961.46(18)
Z	8	2
D_{Calcd} (g cm^{-3})	1.542	1.433
μ (mm^{-1})	1.139	8.070
F(0 0 0)	3024	868.0
Crystal size (mm)	0.14 × 0.14 × 0.12	0.3 × 0.2 × 0.06
2*θ* range for data collection	1.84–27.88	7–144.6
Index ranges	$-34 \le h \le 34$ $-15 \le k \le 16$ $-25 \le l \le 25$	$-16 \le h \le 13$ $-15 \le k \le 18$ $-18 \le l \le 17$
Reflections collected	56,797	15,279
Independent reflections	7609 [R_{int} = 0.0508]	7570 [R_{int} = 0.0393]
Data/restraints/parameters	7609/0/407	7570/0/469
Goodness-of-fit on F^2	1.109	1.024
R/*wR* [$I \ge 2\sigma(I)$]	0.0386/0.0787	0.0452/0.1120
R/*wR* (all data)	0.0432/0.0808	0.0609/0.1238
Max./min. Δ*ρ* (e Å^{-3})	0.340/−0.329	0.69/−0.35

whereas **2** showed an irreversible reduction at −2.061 V and two irreversible oxidation processes at −0.041 and +0.184 V, respectively. Compared with those of parent complex **A** (reduction process at −1.559 V and oxidation process at +0.854 V, figure 3), the oxidation and reduction potentials of **1** shifted 350 and 162 mV negatively, due to one carbonyl being replaced by a stronger electron-donating ligand. For **2**, the corresponding negative shifts are 886 and 502 mV, consistent with the displacement of two carbonyls by dppv. These are characteristic of replacements of carbonyl for phosphine-containing ligands [44]. Compared with the redox potentials of $[(\mu\text{-}SCH_2)_2CHC_6H_5]Fe_2(CO)_5(PPh_3)$ [27], slightly positive shifts (*ca.* 40 mV) were observed for oxidation and reduction potentials of **1**, as do the redox potentials of **2** *versus* those of $[(\mu\text{-}SCH_2)_2CHC_6H_5]Fe_2(CO)_4(\kappa^2\text{-dppv})$ [38]. These observations hint that the electron-withdrawing benzoate on the propanedithiolate has weak influence on the diiron center, different from an electron-withdrawing group attached to 1,2-benzenedithiolate [45–48].

Cyclic voltammetry scans of both complexes were investigated using CF_3COOH (pKa = 12.7 in MeCN) as proton source because the acidity of CF_3COOH is medium and it does not decompose the Fe_2S_2 core. As shown in figure 4, upon addition of 1 equivalent of acid, a new reduction potential appeared at −1.623 V for **1** and the height of this reduction peak increased remarkably as further increments of acid, reaching to *ca.* 160 μA at −1.751 V in the presence of 10 equivalent of acid. Analogous results were also observed for **2** with a new reduction potential appearing at −1.659 V and the height of this reduction peak reaching to 200 μA at −1.926 V (figure 5). The increment of reduction current at −1.623 V for **1** or at −1.659 V for **2** following the further increment of acid is ascribed to

Table 2. Selected bond lengths (Å) and angles (°) for **1** and **2**.

1							
Fe(1)–Fe(2)	2.5341(4)	Fe(1)–S(2)	2.2563(5)	Fe(1)–S(1)	2.2631(6)	Fe(2)–P(1)	2.2486(6)
Fe(2)–S(1)	2.2574(6)	Fe(2)–S(2)	2.2699(6)	Fe(1)–C(1)	1.794(2)	Fe(2)–C(4)	1.779(2)
O(6)–C(8)	1.469(2)	O(6)–C(9)	1.358(2)	O(7)–C(9)	1.204(3)	O(1)–C(1)	1.142(3)
O(5)–C(5)	1.147(3)	O(4)–C(4)	1.148(2)	O(2)–C(2)	1.145(3)	O(3)–C(3)	1.146(2)
Fe(2)–S(1)–Fe(1)	68.192(17)	Fe(1)–S(2)–Fe(2)	68.093(16)	S(2)–Fe(1)–S(1)	84.903(19)	S(1)–Fe(2)–S(2)	84.72(2)
C(1)–Fe(1)–Fe(2)	142.52(7)	P(1)–Fe(2)–Fe(1)	156.02(2)	C(4)–Fe(2)–P(1)	90.54(7)	C(5)–Fe(2)–P(1)	98.74(7)
C(1)–Fe(1)–S(2)	102.35(7)	C(3)–Fe(1)–S(2)	152.55(7)	C(1)–Fe(1)–S(1)	95.44(7)	C(3)–Fe(1)–S(1)	88.73(7)
P(1)–Fe(2)–S(2)	115.81(2)	P(1)–Fe(2)–S(1)	103.14(2)	C(2)–Fe(1)–Fe(2)	110.34(7)	C(3)–Fe(1)–Fe(2)	98.51(7)
S(2)–Fe(1)–Fe(2)	56.208(15)	S(1)–Fe(1)–Fe(2)	55.798(15)	O(6)–C(9)–C(10)	111.78(18)	O(7)–C(9)–O(6)	123.38(19)
2							
Fe(1)–Fe(2)	2.5472(7)	Fe(1)–S(2)	2.2698(10)	Fe(1)–S(1)	2.2657(10)	Fe(2)–P(1)	2.2056(9)
Fe(2)–S(1)	2.2648(9)	Fe(2)–S(2)	2.2586(9)	Fe(1)–C(1)	1.799(4)	Fe(2)–P(2)	2.1974(10)
O(6)–C(34)	1.198(5)	O(5)–C(34)	1.342(5)	O(4)–C(4)	1.148(4)	Fe(2)–C(4)	1.752(3)
Fe(2)–S(1)–Fe(1)	68.42(3)	Fe(1)–S(2)–Fe(2)	68.45(3)	S(2)–Fe(1)–S(1)	84.36(3)	S(1)–Fe(2)–S(2)	84.63(3)
C(1)–Fe(1)–Fe(2)	147.98(14)	P(1)–Fe(2)–Fe(1)	111.54(3)	P(1)–Fe(2)–P(1)	86.62(4)	C(17)–P(1)–Fe(2)	106.21(13)
C(18)–P(2)–Fe(2)	106.80(13)	O(6)–C(34)–C(5)	123.5(4)	O(5)–C(34)–C(35)	112.2(4)	C(34)–O(5)–C(33)	116.3(3)

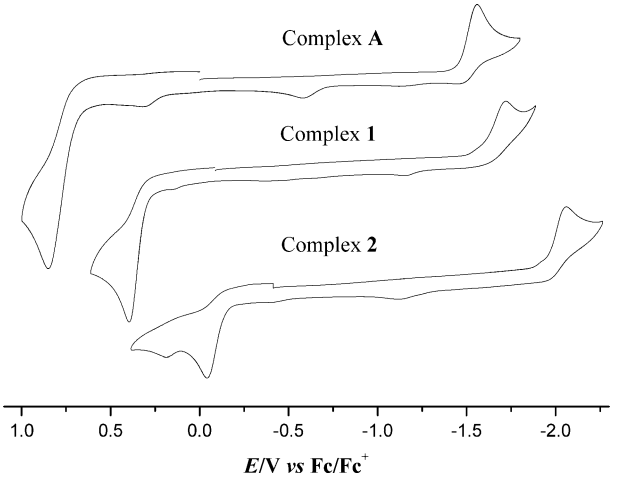

Figure 3. Cyclic voltammetry of **A**, **1** and **2** (1 mmol) in 0.1 M *n*-Bu_4NPF_6/MeCN at a scan rate of 0.1 V s^{-1}.

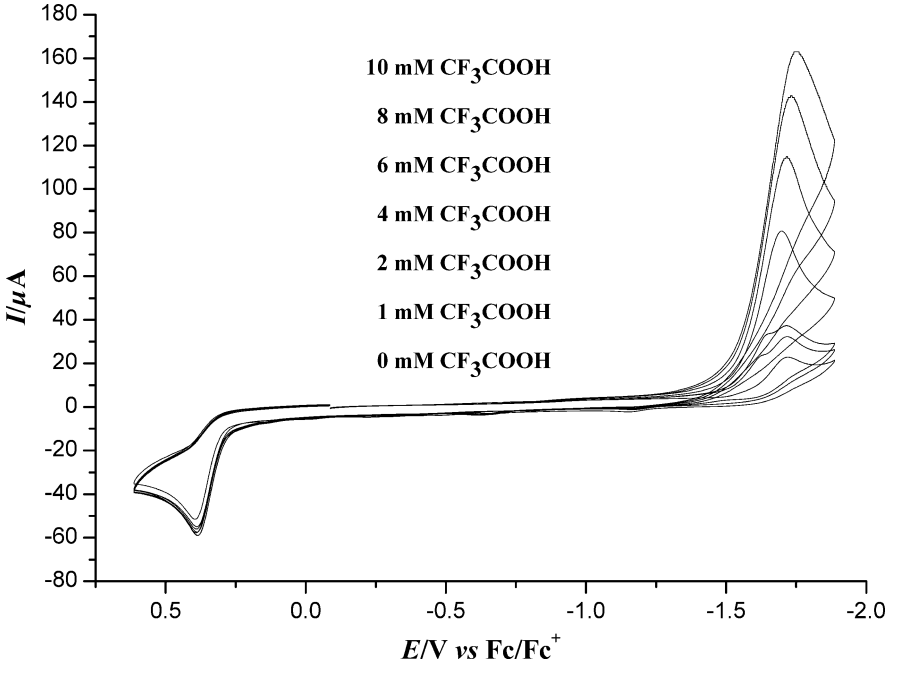

Figure 4. Cyclic voltammetry of **1** (1 mmol) in 0.1 M *n*-Bu_4NPF_6/MeCN under CF_3COOH (0–10 mmol) at a scan rate of 0.1 V s^{-1}.

catalytic reduction of protons [49–52]. The catalytic reduction currents of **2** were larger than those of **1** in the presence of the same concentration of acid, showing **2** to be an effective catalyst of reduction of protons and confirming the conclusion of Tye et al. [29].

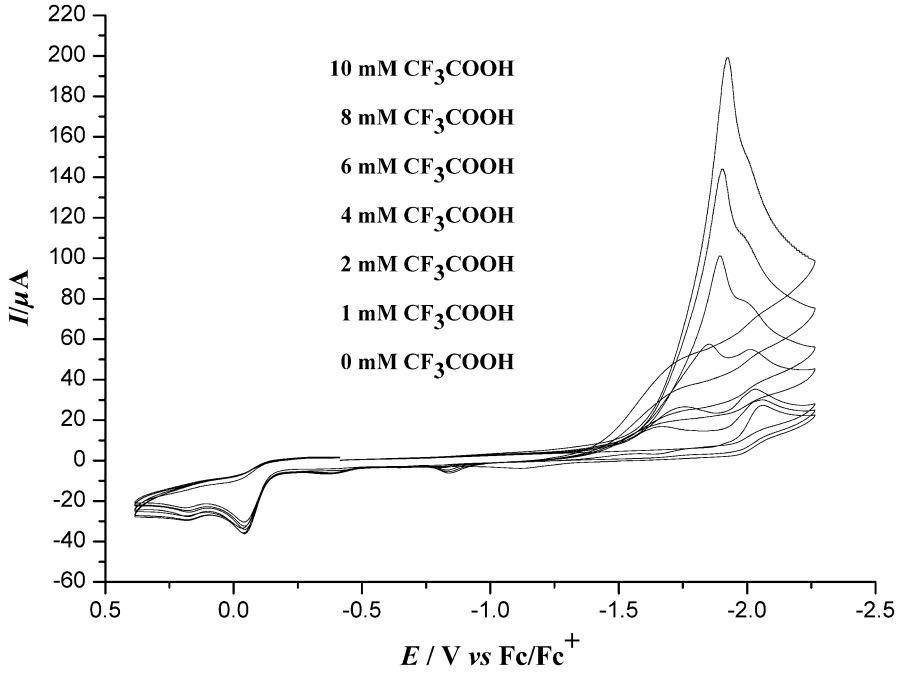

Figure 5. Cyclic voltammetry of **2** (1 mmol) in 0.1 M n-Bu_4NPF_6/MeCN under CF_3COOH (0–10 mmol) at a scan rate of 0.1 V s^{-1}.

4. Conclusion

Displacement of one or two carbonyls of benzoate-functionalized all-carbonyl diiron propanedithiolate [μ-$(SCH_2)_2CHO_2CC_6H_5]Fe_2(CO)_6$ by a unidentate or bidentate phosphine yielded a mono-substituted complex [μ-$(SCH_2)_2CHO_2CC_6H_5]Fe_2(CO)_5(PPh_3)$ or a chelated complex [(μ-$SCH_2)_2CHO_2CC_6H_5]Fe_2(CO)_4(\kappa^2$-dppv). Compared with phenyl-functionalized diiron propanedithiolate complex [μ-$(SCH_2)_2CHC_6H_5]Fe_2(CO)_5(PPh_3)$ and [(μ-$SCH_2)_2CHC_6H_5]Fe_2(CO)_4(\kappa^2$-dppv), electron-withdrawing benzoate positively shifted the oxidation and reduction potentials of diiron centers slightly (*ca.* 40 mV). Both complexes can catalyze the reduction of protons from CF_3COOH to hydrogen, of which the chelated complex had a higher catalytic efficiency.

Supplementary material

Crystallographic data for the structures reported in this article have been deposited with the Cambridge Crystallographic Data Center as supplementary publication Nos. CCDC 953987 (**1**) and 1021174 (**2**). Copies of the data can be obtained free of charge via www.ccdc.cam.ac.uk (or from the Cambridge Crystallographic Center, 12 Union Road, Cambridge CB2 1EZ, UK; Fax: +44 1223 336033; E-mail: deposit@ccdc.cam.ac.uk).

Disclosure statement

No potential conflict of interest was reported by the authors.

Funding

This work was supported by the Chinese National Natural Science Foundation [grant number 21072046]; the Chinese National Training Programs of Innovation and Entrepreneurship for Undergraduates [grant number 201210467022].

References

[1] D. Das, V.T. Nejat. *Int. J. Hydrogen Energy*, **26**, 13 (2001).
[2] N.Z. Muradov, T.N. Veziroglu. *Int. J. Hydrogen Energy*, **33**, 6804 (2008).
[3] M. Frey. *ChemBioChem*, **3**, 153 (2002).
[4] J.W. Peters, W.N. Lanzilotta, B.J. Lemon. *Science*, **282**, 1853 (1998).
[5] Y. Nicolet, C. Piras, P. Legrand, C.E. Hatchikian, J.C. Fontecilla-Camps. *Structure*, **7**, 13 (1999).
[6] Y. Nicolet, A.L. de Lacey, X. Vernède, V.M. Fernandez, E.C. Hatchikian, J.C. Fontecilla-Camps. *J. Am. Chem. Soc.*, **123**, 1596 (2001).
[7] A.J. Pierik, M. Hulstein, W.R. Hagen, S.P.J. Albracht. *Eur. J. Biochem.*, **258**, 572 (1998).
[8] A.L. De Lacey, C. Stadler, C. Cavazza, E.C. Hatchikian, V.M. Fernandez. *J. Am. Chem. Soc.*, **122**, 11232 (2000).
[9] D.W. Mulder, M.W. Ratzloff, E.M. Shepard, A.S. Byer, S.M. Noone, J.W. Peters, J.B. Broderick, P.W. King. *J. Am. Chem. Soc.*, **135**, 6921 (2013).
[10] F. Gloaguen, T.B. Rauchfuss. *Chem. Soc. Rev.*, **38**, 100 (2009).
[11] I.P. Georgakaki, L.M. Thomson, E.J. Lyon, M.B. Hall, M.Y. Darensbourg. *Coord. Chem. Rev.*, **238–239**, 255 (2003).
[12] X.M. Liu, S.K. Ibrahim, C. Tard, C.J. Pickett. *Coord. Chem. Rev.*, **249**, 1641 (2005).
[13] T.R. Simmons, G. Berggren, M. Bacchi, M. Fontecave, V. Artero. *Coord. Chem. Rev.*, **270–271**, 127 (2014).
[14] N. Wang, M. Wang, L. Chen, L.C. Sun. *Dalton Trans.*, **42**, 12059 (2013).
[15] D.J. Evans, C.J. Pickett. *Chem. Soc. Rev.*, **32**, 268 (2003).
[16] C. Tard, C.J. Pickett. *Chem. Rev.*, **109**, 2245 (2009).
[17] M. Wang, L. Chen, L.C. Sun. *Energy Environ. Sci.*, **5**, 6763 (2012).
[18] A. Winter, L. Zsolnai, G. Huttner. *Z. Naturforsch., B: Chem. Sci.*, **37**, 1430 (1982).
[19] L.C. Song, C.G. Li, J. Gao, B.S. Yin, X. Luo, X.G. Zhang, H.L. Bao, Q.M. Hu. *Inorg. Chem.*, **47**, 4545 (2008).
[20] S. Salyi, M. Kritikos, B. Åkermark, L.C. Sun. *Chem. Eur. J.*, **9**, 557 (2003).
[21] L.C. Song, L.X. Wang, C.G. Li, F.Y. Li, Z.F. Chen. *J. Organomet. Chem.*, **749**, 120 (2014).
[22] L.C. Song, W. Gao, X. Luo, Z.X. Wang, X.J. Sun, H.B. Song. *Organometallics*, **31**, 3324 (2012).
[23] C.M. Thomas, O. Rüdiger, T.B. Liu, C.E. Carson, M.B. Hall, M.Y. Darensbourg. *Organometallics*, **26**, 3976 (2007).
[24] P.H. Zhao, Y.Q. Liu, G.Z. Zhao. *Polyhedron*, **53**, 144 (2013).
[25] P.H. Zhao, Y.F. Liu, K.K. Xiong, Y.Q. Liu. *J. Cluster Sci.*, **25**, 1061 (2014).
[26] M.L. Singleton, R.M. Jenkins, C.L. Klemashevich, M.Y. Darensbourg. *C.R. Chim.*, **11**, 861 (2008).
[27] C.G. Li, Y. Zhu, X.X. Jiao, X.Q. Fu. *Polyhedron*, **67**, 416 (2014).
[28] L.C, Song, L.X. Wang, G.J. Jia, Q.L. Li, J.B. Ming. *Organometallics*, **31**, 5081 (2012).
[29] J.W. Tye, M.Y. Darensbourg, M.B. Hall. *Inorg. Chem.*, **45**, 1552 (2006).
[30] O.V. Dolomanov, L.J. Bourhis, R.J. Gildea, J.A.K. Howard, H. Puschmann. *J. Appl. Crystallogr.*, **42**, 339 (2009).
[31] G.M. Sheldrick. *Acta Crystallogr. Sect. A: Found. Crystallogr.*, **64**, 112 (2008).
[32] L.J. Luo, X.F. Liu, H.Q. Gao. *J. Coord. Chem.*, **66**, 1077 (2014).
[33] X.F. Liu, X. Lia. *J. Coord. Chem.*, **67**, 3266 (2014).
[34] W.M. Gao, J. Ekström, J.H. Liu, C.N. Chen, L. Eriksson, L.H. Weng, B. Åkermark, L.C. Sun. *Inorg. Chem.*, **46**, 1981 (2007).
[35] P. Li, M. Wang, C.J. He, G.H. Li, X.Y. Liu, C.N. Chen, B. Åkermark, L.C. Sun. *Eur. J. Inorg. Chem.*, 2506 (2005).
[36] A.K. Justice, G. Zampella, L. De Gioia, T.B. Rauchfuss, J.I. van der Vlugt, S.R. Wilson. *Inorg. Chem.*, **46**, 1655 (2007).
[37] F.I. Adam, G. Hogarth, I. Richards. *J. Organomet. Chem.*, **692**, 3957 (2007).
[38] C.G. Li, Y.F. Li, J.Y. Shang, T.J. Lou. *Transition Met. Chem.*, **39**, 373 (2014).

[39] P.H. Zhao, X.H. Li, Y.F. Liu, Y.Q. Liu. *J. Coord. Chem.*, **67**, 766 (2014).
[40] M.N. Burnett, C.K. Johnson. ORTEP-III: Oak Ridge Thermal Ellipsoid Plot Program for Crystal Structure Illustrations, Oak Ridge National Laboratory Report ORNL-6895, Oak Ridge, TN (1996).
[41] Z. Wang, W.F. Jiang, J.H. Liu, W.N. Jiang, Y. Wang, B. Åkermark, L.C. Sun. *J. Organomet. Chem.*, **693**, 2828 (2008).
[42] Z.B. Zhao, M. Wang, W.B. Dong, P. Li, Z. Yu, L.C. Sun. *J. Organomet. Chem.*, **694**, 2309 (2009).
[43] X.F. Liu, X.W. Xiao. *J. Organomet. Chem.*, **696**, 2767 (2011).
[44] G.A.N. Felton, C.A. Mebi, B.J. Petro, A.K. Vannucci, D.H. Evans, R.S. Glass, D.L. Lichtenberger. *J. Organomet. Chem.*, **694**, 2681 (2009).
[45] L. Schwartz, P.S. Singh, L. Eriksson, R. Lomoth, S. Ott. *C.R. Chim.*, **11**, 875 (2008).
[46] K. Charreteur, M. Kdider, J.F. Capon, F. Gloaguen, F.Y. Pétillon, P. Schollhammer, J. Talarmin. *Inorg. Chem.*, **49**, 2496 (2010).
[47] F. Ridley, S. Ghosh, G. Hogarth, N. Hollingsworth, K.B. Holt, D.G. Unwin. *J. Electroanal. Chem.*, **703**, 14 (2013).
[48] L. Schwartz, L. Eriksson, R. Lomoth, F. Teixidor, C. Viñas, S. Ott. *Dalton Trans.*, 2379 (2008).
[49] D. Chong, I.P. Georgakaki, R. MejiaRodriguez, J. Sanabria-Chinchilla, M.P. Soriaga, M.Y. Darensbourg. *Dalton Trans.*, 4158 (2003).
[50] S.J. Borg, T. Behrsing, S.P. Best, M. Razavet, X.M. Liu, C.J. Pickett. *J. Am. Chem. Soc.*, **126**, 16988 (2004).
[51] F. Gloaguen, J.D. Lawrence, T.B. Rauchfuss. *J. Am. Chem. Soc.*, **123**, 9476 (2001).
[52] J.F. Capon, F. Gloaguen, F.Y. Pétillon, P. Schollhammer, J. Talarmin. *Coord. Chem. Rev.*, **253**, 1476 (2009).